*Computers and Concrete, Vol. 5, No. 4 (2008) 279-293* 
DOI: http://dx.doi.org/10.12989/cac.2008.5.4.279

# Numerical analysis of spalling of concrete cover at high temperature

Joško Ožbolt*, Goran Periškić, Hans-Wolf Reinhardt and Rolf Eligehausen

*Institute for Construction Materials Stuttgart, Germany*

*(Received November 1, 2007, Accepted April 1, 2008)*

**Abstract.** In the present paper a 3D thermo-hygro-mechanical model for concrete is used to study explosive spalling of concrete cover at high temperature. For a given boundary conditions the distribution of moisture, pore pressure, temperature, stresses and strains are calculated by employing a three-dimensional transient finite element analysis. The used thermo-hygro-mechanical model accounts for the interaction between hygral and thermal properties of concrete. Moreover, these properties are coupled with the mechanical properties of concrete, i.e., it is assumed that the mechanical properties (damage) have an effect on distribution of moisture (pore pressure) and temperature. Stresses in concrete are calculated by employing temperature dependent microplane model. To study explosive spalling of concrete cover, a 3D finite element analysis of a concrete slab, which was locally exposed to high temperature, is performed. It is shown that relatively high pore pressure in concrete can cause explosive spalling. The numerical results indicate that the governing parameter that controls spalling is permeability of concrete. It is also shown that possible buckling of a concrete layer in the spalling zone increases the risk for explosive spalling.

**Keywords:** concrete; high temperature; explosive spalling; thermo-hygro-mechanical model; microplane model; finite elements.

## 1. Introduction

When temperature increases for a couple of hundred of degrees Celsius, behaviour of concrete changes significantly. The concrete mechanical properties, such as strength, Young's modulus and fracture energy, are at high temperatures rather different than for concrete at normal temperatures. At high temperature large temperature gradients lead in concrete structures to temperature-induced stresses, which cause damage. Furthermore, creep and relaxation of concrete that is due to high temperature play also an important role. One of the reasons for the complexity of the behaviour of concrete at high temperatures is due to the fact that concrete contains water, which changes its state of aggregation at high temperature and can generate significant pore pressure. Furthermore, the microstructure of concrete is extremely complex and at high temperature there are chemical changes which significantly influence overall properties of concrete. Moreover, at high temperature the aggregate can change its structure or it can loose its weight through the emission of $CO_2$, such as calcium-based stones. Consequently, the behaviour of concrete at high temperature depends strongly on concrete type.

* Corresponding author E-mail: ozbolt@iwb.uni-stuttgart.de

Although the behaviour of concrete at high temperature is in the literature well documented (Thelandersson 1983, Khoury, *et al*. 1985, Schneider 1986, Bažant and Kaplan 1996, Zhang and Biani 2002, Khoury 2006, Zieml, *et al*. 2006) further experimental and theoretical studies are needed to clarify the interaction between hygro-thermal and mechanical properties, such as for instance explosive type of failure due to spalling of concrete cover. The main problem in the experimental investigations is that such experiments are rather demanding, i.e., one has to perform loading and measurement at extremely high temperatures. Furthermore, such experiments can be carried out only on relatively small structures. To better understand the behaviour of concrete at high temperature and to support the experiments, numerical analysis can be useful. However, one needs models, which can realistically predict behaviour of concrete at high temperatures.

In the last two decades significant advancement has been achieved in the modelling of behaviour of concrete at high temperatures (Bažant and Kaplan 1996, Gawin, *et al*. 1999, 2006, Tenchev, *et al*. 2001, Nielsen, *et al*. 2002, Ožbolt, *et al*. 2005). There are principally two groups of phenomenological models: (i) Thermo-mechanical models and (ii) Thermo-hygro-mechanical models. In the first group, the mechanical properties of concrete are temperature- (moisture-) dependent whereas the temperature (moisture) distribution is independent of the mechanical properties of concrete. The second group of models are from the physical point of view more realistic. Namely, in these models the physical processes, which take place in concrete, are coupled, i.e., the interaction between mechanical properties, temperature, moisture, pore pressure and hydration of concrete is accounted for. Note that in both group of models the chemical changes of concrete at high temperature are usually implicitly accounted for.

In the modelling of concrete at high temperature there are two important aspects that are relevant for the realistic prediction of concrete behaviour at high temperature: (i) description of the state of pore water in concrete and (ii) mechanical constitutive law for concrete. As will be discussed later, in the present paper a relatively simple, single phase model for description of state of pore water in concrete is employed (Bažant and Thonguthai 1978). The main argument for the use of this approach is its relative simplicity. The approach is principally based on irreversible thermodynamics, which is combined with experimental results. The advantage is that there are not too many parameters and they can be relatively easily obtained from experiments. Further argument for the use of such a model may possibly be due to the fact that in the modelling of complex processes, which take place at the micro-structural level of concrete, the theory must be corrected by experimental results.

The models with a more general physical background (multi-phase models) are more complex (Gawin, *et al*. 1999, 2006, Tenchev, *et al*. 2001). In such models there are a number of parameters, which can not be obtained directly from experiments. The multi-scale approach is needed to calibrate the parameters of the model and subsequently a homogenisation strategy should be employed to be able to use these parameters in the macroscopic continuum analysis. Having on mind a number of assumptions that are needed in these models, it is impossible to state that such a model would result in a more realistic prediction of behaviour of concrete at high temperatures than the prediction of a single phase model used in the present paper.

In the present paper, a three-dimensional (3D) model based on thermo-hygro-mechanical coupling between thermo (temperature), hygro (moisture and pore pressure) and mechanical properties of concrete is discussed. The temperature-dependent microplane model (Ožbolt, *et al*. 2005) is used as a constitutive law for concrete with model parameters being made temperature-dependent. The model is implemented into a three-dimensional finite element (FE) code and subsequently, the problem of spalling of concrete cover at high temperatures is investigated. The finite element analysis is incremental, i.e., it is performed through a number of loading (time) steps. For given temperature, humidity and loading boundary conditions, in each time step moisture, pore pressure, temperature, stresses and strains are simultaneously calculated. The time integration is based on an implicit iterative scheme. The numerical results presented in the present paper should be considered as preliminary. Namely, because of the complexity of the problem, further work is needed to verify the model performance in more detail.

## 2. Thermo-hygro-mechanical model for concrete

The present phenomenological model for concrete is a thermo-hygro-mechanical. It is formulated in the framework of continuum mechanics under the assumption of validity of irreversible thermodynamics. The response of the model is controlled by the following unknowns: temperature, pore pressure (moisture), stresses and strains. The distribution of temperature, pore pressure and moisture (thermo-hygral properties) depends on damage of concrete. Moreover, the relevant macroscopic mechanical properties (Young's modulus, tensile strength, compressive strength and fracture energy) are temperature-dependent.

### *2.1. Coupled heat and moisture transfer*

The general approach for the solution of the problem of coupled heat and mass transfer in a porous solid such as concrete, within the framework of irreversible thermodynamics, is well known. However, there are a number of complex details and, therefore, for the practical application the problem must be simplified (Bažant and Thonguthai 1978). Assuming for a moment that the moisture flux (**J**) and heat flux (**q**) in concrete are stress and strain independent, the following is valid (Bažant and Thonguthai 1978):

$$\mathbf{J} = -\, a_{ww}\, grad\, w - a_{wT}\, grad\, T \tag{1}$$

$$\mathbf{q} = -\, a_{Tw}\, grad\, w - a_{TT}\, grad\, T \tag{2}$$

where $a_{ww}$, $a_{TT}$, $a_{wT}$ and $a_{Tw}$ are coefficients, which depend on the evaporable water content $w$ and temperature $T$. Water content $w$ is a function of $T$ and pore pressure $p$. Assuming that $a_{wT}$ and $a_{Tw}$ have relatively small contribution and replacing $w$ with $p$, Eqs. (1) and (2) can be rewritten as:

$$\mathbf{J} = -\, a\, grad\, p \tag{3}$$

$$\mathbf{q} = -\, b\, grad\, T \tag{4}$$

with $a$ = permeability [m/s] and $b$ = heat conductivity. Note, that $a$ is not intrinsic permeability, which depends only on porosity, it is relative permeability that depends on temperature, pore pressure and saturation of concrete (saturated or non-saturated). As will be discussed later, $a$ is obtained from sorption isotherms.

Using the condition of conservation of mass and Eq. (3) it follows:

$$\frac{\partial w}{\partial t} = -div\mathbf{J} + \frac{\partial w_d}{\partial t} \tag{5}$$

where $t$ = time and $w_d$ = total mass of water released into the pore by dehydration. In the present model dehydration is not accounted for. The balance of heat together with Eq. (4) requires:

$$C\rho\frac{\partial T}{\partial t}-C_a\frac{\partial w}{\partial t}-C_w\frac{\partial T}{\partial t}\mathbf{J}\ grad\ T=-div\ \mathbf{q} \tag{6}$$

where $\rho$ = mass density and $C$ = isobaric heat capacity of concrete that includes chemically bounded water, but excluding free water, $C_a$ = heat sorption of free water and $C_w$ = heat capacity of water, which is in the present model neglected. The first member of the left hand side of Eq. 6 is the contribution of change of temperature to heat, the second one is the contribution of free water to heat in concrete and the third member is due to heat convection of moving water in concrete which is usually important at high heating rates.

Boundary conditions at concrete surface are defined as:

$$\mathbf{n}\cdot\mathbf{J}=\alpha_w\,(p_0-p_E) \tag{7}$$

$$\mathbf{n}\cdot\mathbf{q}=\alpha_G\,(T_0-T_E) \tag{8}$$

where $\alpha_w$ = surface emissivity of water, $\alpha_G$ = surface emissivity of heat, $T_0$ and $p_0$ are temperature and pore pressure at concrete surface and $T_E$ and $p_E$ are temperature and pore pressure of environment.

### 2.2. State of pore water and permeability

The problem in the above equations is the determination of material properties. Assuming for a moment no stress-dependency, the constitutive laws for $p$, $w$ and $T$ follow simplified suggestions proposed by Bažant and Thonguthai (1978). To describe the state of pore water in concrete, for temperatures below the critical point of water (374.15°C) one has to distinguish three different states: (i) unsaturated concrete – relative pore pressure $h\leq 0.96$, (ii) saturated concrete – relative pore pressure $h\geq 1.04$ and (iii) transition from unsaturated to saturated concrete − $0.96 < h < 1.04$. The difficulty here is that by increasing temperature the properties of concrete significantly change. The state equations follow known theoretical background, however, due the complexity of concrete structure, the change of its thermo-hygro-mechanical properties at macro scale (continuum) is most probably impossible to describe by explicit laws. Therefore, to obtain realistic prediction for heated concrete the controlling parameters had to be fitted by available test data (Bažant and Thonguthai 1978).

Because the theoretical solution is based on simplified assumptions, no change of pore geometry and the amount of adsorbed water is negligible, it must be empirically corrected. Consequently, according to the model proposed by Bažant and Thonguthai (1978), for unsaturated concrete ($p\leq p_s$, $p_s$ = saturation pressure) the state of pore water reads:

$$\frac{w}{c}=\left(\frac{w_1}{c}h\right)^{1/(m(T))}\quad\text{with}\quad h=\frac{p}{p_s(T)},\ h\leq 0.96 \tag{9}$$

$$\text{with}\ \ m(T)=1.04-\frac{T'}{22.34+T'};\ T'=\left(\frac{T+10}{T_0+10}\right)^2 \tag{10}$$

where $T$ = temperature in °C, $T_0$ = 25°C, $c$ = mass of cement per m$^3$ of concrete and $w_1$ = saturation water content at 25°C.

For saturated concrete one can theoretically calculate $p$ for a given $w$ and $T$ by using steam tables. However, this would, already for relative low temperatures, yield to extremely high pore pressure, which is not realistic. Porosity of concrete $n$ at higher temperatures increases because of dehydration and chemical changes of cement paste (Bažant and Cusatis 2005). Therefore, to account for these effects, the initial porosity of concrete $n_0$ has to be corrected by an empirical correction function (Bažant and Thonguthai 1978):

$$n = \left(n_0 + \frac{w_d(T) - w_{d0}}{\rho_0}\right) P(h) \quad \text{for } h \geq 1.04 \tag{11}$$

$$P(h) = 1 + 0.12(h - 1.04)\,,\ h = \frac{p}{p_s(T)} \tag{12}$$

Function $P(h)$ is identified by fitting of test data and $w_d(T)$ is taken from the measurements of weight loss of specimens of heated concrete in thermodynamic equilibrium (Harmathy and Allen 1973). Using Eq. 11 and 12, the water content in saturated concrete can be calculated as:

$$w = (1 + 3\varepsilon^v)\frac{n}{v} \quad \text{with } d\varepsilon^v = \frac{d\sigma^v}{3K} + \alpha_T dT\,,\ \sigma^v = np \tag{13}$$

in which $\varepsilon^v$ = volumetric strain due to the resulting volumetric stress $\sigma^v$ caused by pore pressure, $v$ = specific volume of water, $K$ = bulk modulus and $\alpha_T$ = coefficient of linear thermal expansion of concrete.

The transition from unsaturated to saturated concrete can be abrupt only for an extremely slow change in pore pressure. For most practical situations the transition is most likely smooth. Furthermore, an abrupt transition would cause numerical difficulties. Therefore, for relative humidity $h$ between 0.96 and 1.04 and for a given temperature $T$, linear increase of free water content from unsaturated state ($h$ = 0.96) to saturated state ($h$ = 1.04) is assumed (Bažant and Thonguthai 1978).

The permeability function for concrete also follows suggestions proposed by Bažant and Thonguthai (1978). Due to the fact that permeability of concrete above 100°C increases by about two orders of magnitude, a function which controls permeability consists of two parts – for $T \leq$ 95°C and for $T >$ 95°C:

$$a = a_0 f_1(h) f_2(T) \quad \text{for } T \leq 95^\circ\text{C}$$

$$a = a_0^* f_3(T) \quad \text{for } T > 95^\circ\text{C with } a_0^* = a_0 f_2(95^\circ\text{C}) \tag{14}$$

in which $a_0$ is the reference permeability at 25°C. Function $f_1(h)$ reflects the moisture transfer within the adsorbed water layers in the necks that connect pores in cement gel and according to Bažant and Thonguthai (1978) it reads:

$$f_1(h) = \alpha + \frac{1-\alpha}{1 + \left(\frac{1-h}{1-h_c}\right)^4}\,,\ \text{for } h \leq 1\,;\ f_1(h) = 1,\ \text{for } h \geq 1 \tag{15}$$

where $h_c$ = 0.75 = transition humidity and $\alpha$ = 1/20 at 25°C. The temperature dependence of permeability below 95°C reads (Bažant and Thonguthai 1978):

$$f_2(T) = exp\left[\frac{Q}{R}\left(\frac{1}{T_0} - \frac{1}{T}\right)\right];\ T \leq 95^\circ\text{C} \tag{16}$$

in which $\overline{T}$ = absolute temperature, $Q$ = activation energy for water migration along the adsorption layers in the necks and $R$ = gas constant.

Function $f_3$ should reflect the fact that between 95°C and 105°C there is a transition from the moisture transfer mechanism that is governed by the activation energy of adsorption to a mechanism that is governed by viscosity of a mixture of liquid water and steam. This property can be described as (Bažant and Thonguthai 1978):

$$f_3(T) = exp\left[\frac{T-95}{0.881+0.214(T-95)}\right];\ T > 95^{\circ}\mathrm{C} \tag{17}$$

where $T$ is in °C. For more detail related to the physical background of Eqs. (14) to (17) see Bažant and Thonguthai (1978).

### *2.3. Thermo-mechanical coupling*

In the mechanical part of the model the total strain tensor for stressed concrete exposed to high temperature is decomposed as (Khoury, *et al*. 1985, Neilsen, *et al*. 2002):

$$\boldsymbol{\varepsilon} = \boldsymbol{\varepsilon}^{m}(T,\boldsymbol{\sigma})+\boldsymbol{\varepsilon}^{ft}(T)+\boldsymbol{\varepsilon}^{tm}(T,\boldsymbol{\sigma})+\boldsymbol{\varepsilon}^{c}(T,\boldsymbol{\sigma}) \tag{18}$$

where $\boldsymbol{\varepsilon}^{m}$ = mechanical strain tensor, $\boldsymbol{\varepsilon}^{ft}$ = free thermal strain tensor, $\boldsymbol{\varepsilon}^{tm}$ = thermo-mechanical strain tensor and $\boldsymbol{\varepsilon}^{c}$ is strain that is due to the temperature dependent creep of concrete. In the following the strain components are only briefly discussed. For more detail see Ožbolt, *et al*. (2005).

The mechanical strain tensor $\boldsymbol{\varepsilon}^{m}$, that comes into the 3D constitutive law for concrete (microplane model), is calculated as $\boldsymbol{\varepsilon}^{m} = \boldsymbol{\varepsilon} - (\boldsymbol{\varepsilon}^{ft} + \boldsymbol{\varepsilon}^{tm} + \boldsymbol{\varepsilon}^{c})$. The mechanical strains are then used to calculate the effective stresses increments $\dot{\overline{\boldsymbol{\sigma}}}$ (stress in solid phase of concrete matrix) and macroscopic stresses increments $\dot{\boldsymbol{\sigma}}$ from the microplane constitutive law (Ožbolt, *et al*. 2001, Ožbolt, *et al*. 2005):

$$\dot{\boldsymbol{\sigma}} = \mathbf{D}:\dot{\boldsymbol{\varepsilon}}^{m}+\dot{\boldsymbol{\sigma}}^{p} \tag{19}$$

in which $\mathbf{D}$ = tangent material stiffness tensor obtained from the microplane model, $\dot{\boldsymbol{\varepsilon}}^{m}$ = increment of the mechanical strain and $\dot{\boldsymbol{\sigma}}^{p}$ = increment of pore pressure, which is calculated from the increment of volumetric pore pressure $\dot{\boldsymbol{\sigma}}^{v} = n\dot{p}$, with $\dot{p}$ = increment of pore pressure. Note, that according to definition pore pressure $p$ is negative. In general, the mechanical strain component can be decomposed into elastic, plastic and damage part. The sources of mechanical strains are external load, thermal strain induced stress and pore pressure in concrete.

The parameters of the microplane model are modified such that the macroscopic response of the model fits temperature-dependent mechanical properties of the concrete (Ožbolt, *et al*. 2005). To account for finite strains the co-rotational stress tensor together with logarithmic strain tensor (Belytschko, *et al*. 2001) are used in the formulation of the microplane model. The finite strain formulation is needed in order to investigate the influence of geometrical instabilities of concrete layer (buckling) on explosive type of spalling of concrete cover. Free thermal strain is stress-independent and it is experimentally obtained by measurements on a load-free specimen. The total free thermal strain consists of temperature dilatation and shrinkage of concrete, which can be experimentally isolated (Khoury 2006). In the presented model the temperature-dependent shrinkage is a part of the free thermal strain. The thermo-mechanical strain is stress and temperature dependent. It appears only during first heating and not during subsequent cooling and heating cycles (Khoury, *et al*. 1985, Khoury 2006). This strain is irrecoverable and leads in concrete structures to severe tensile stresses during cooling. Temperature-dependent creep strain is of the same nature as the thermo-mechanical strain except that it is partly recoverable. In an experiment it is not possible to isolate this strain. For low temperature rate, which is normal case in the experiments, this strain component compared to the thermo-mechanical strain is small. Therefore, temperature dependent creep strain is in the present model neglected.

### *2.4. Thermo-hygro-mechanical coupling*

Thermo-hygro processes are coupled with mechanical properties of concrete in both directions. It is known that permeability and porosity of concrete are relevant parameters that control transport processes in concrete. On the other hand, both porosity and permeability are influenced by damage, i.e., for higher level of damage, porosity and permeability of concrete are higher. To account for this, permeability and porosity of concrete are assumed to be stress- (strain-) dependent. Following suggestions from the literature (Wang, *et al*. 1997), the relations plotted in Fig. 1 are adopted in the present model. Crack opening is calculated using temperature-dependent microplane model (Ožbolt, *et al*. 2005).

From Fig. 1(a) it can be seen that after crack opening reaches a threshold value $\alpha_a \cdot cw_c$, permeability of concrete increases up to its maximal value ($1000a_{cw=0} \times 103$) that is reached at critical crack width. For further increase of the crack width (open crack), permeability is assumed to be constant. Actually, after crack opens one should start to treat the crack surfaces as a free surfaces taking into account special boundary conditions on them. For more detail see for instance work of Therrien and Sudicky (1996). The present model is formulated in the framework of continuum mechanics, therefore, because of numerical reasons it is assumed that permeability in cracked finite element remains constant after it reaches maximal threshold value. Moreover, as soon as a crack fully opens, pore pressure drops almost to zero and permeability becomes less important. The same arguments apply for (see Fig. 1b), which is in cracked finite elements assumed to be constant and equal to 0.8.

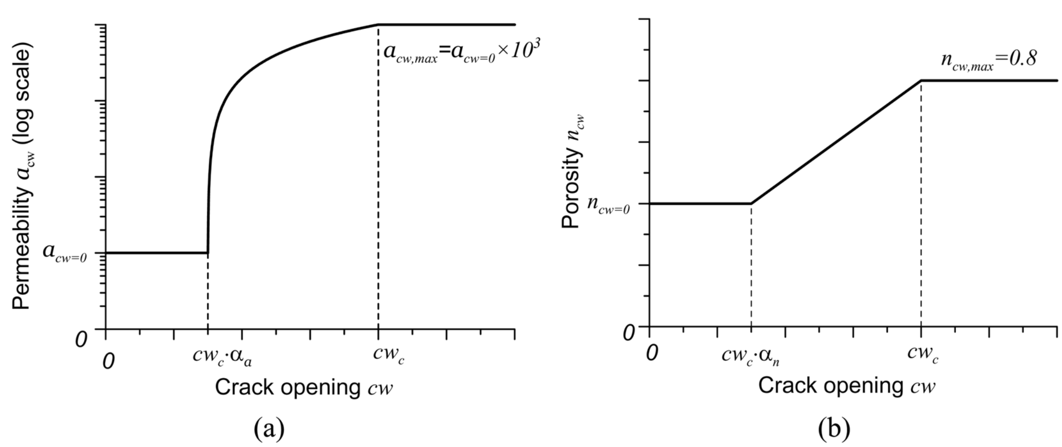


Fig. 1 a) Permeability $a_{cw}$ as a function of a crack width ($1 \geq \alpha_a \geq 0$) and b) porosity $n_{cw}$ as a function of crack width ($1 \geq \alpha_n \geq 0$)

## 3. Numerical implementation

The numerical analysis is incremental. In each time step $\Delta t$ partial differential equations, which control heat and moisture transfer in concrete, and equation of equilibrium (mechanical part of the model) are solved simultaneously. When solving Eqs. (5) and (6) it is assumed that damage is constant, i.e., thermo-hygro properties of concrete are controlled by damage from the end of the previous time step. To solve the problem by the finite element method, Eqs. (5) and (6) have to be rewritten in the weak (integral) form. After introducing stationary condition on the governing functional one obtains the following system of linear equations (Voigt notation):

$$\begin{aligned} [C_1]\{\dot{p}\} + [C_2]\{\dot{T}\} + [K_1]\{p\} &= \{R_1\} \\ [C_3]\{\dot{T}\} + [C_4]\{\dot{p}\} + [K_2]\{T\} &= \{R_2\} \end{aligned} \tag{20}$$

with:

$$[C_1] = \int_\Omega \frac{\partial w}{\partial p}[N]^T[N]d\Omega;\ [C_2] = \int_\Omega \frac{\partial w}{\partial t}[N]^T[N]d\Omega;$$

$$[C_3] = \int_\Omega \left(C\rho - C_a\frac{\partial w}{\partial t}\right)[N]^T[N]d\Omega;\ [C_4] = \int_\Omega -C_a\frac{\partial w}{\partial p}[N]^T[N]d\Omega;$$

$$[K_1] = \int_\Omega a[B]^T[B]d\Omega;\ [K_2] = \int_\Omega b[B]^T[B]d\Omega$$

$$[R_1] = \int_\Gamma [N]^T a_w p_{en} d\Gamma;\ [R_2] = \int_\Gamma [N]^T a_G p_{en} d\Gamma$$

where $[N]$ is the column matrix of shape functions that relates pore pressure (temperature) field with their nodal values and $[B]$ relates the field of pore pressure (temperature) gradients and nodal values.

Eq. (20) is solved using direct integration method based on the following assumption for the solution in the $(r+1)^{\text{th}}$ time step:

$$\begin{aligned} \{p\}_{r+1} &= \{p\}_r + \{(1-\beta)\dot{p}_r + \beta\dot{p}_{r+1}\}\Delta t \\ \{T\}_{r+1} &= \{T\}_r + \{(1-\beta)\dot{T}_r + \beta\dot{T}_{r+1}\}\Delta t \end{aligned} \tag{21}$$

where parameter $\beta$ is set to $\beta = 1.0$, which yields to the unconditionally stable backward difference method that reads (Belytschko, *et al.* 2001):

$$\begin{aligned} \left(\frac{[C_1]}{\Delta t} + [K_1]\right)\{p\}_{r+1} + \frac{[C_2]}{\Delta t}\{T\}_{r+1} &= \frac{[C_1]}{\Delta t}\{p\}_r + \frac{[C_2]}{\Delta t}\{T\}_r + \{R_1\} \\ \left(\frac{[C_3]}{\Delta t} + [K_2]\right)\{T\}_{r+1} + \frac{[C_4]}{\Delta t}\{p\}_{r+1} &= \frac{[C_3]}{\Delta t}\{T\}_r + \frac{[C_4]}{\Delta t}\{p\}_r + \{R_2\} \end{aligned} \tag{22}$$

In Eq. (20) the controlling parameters are coupled, therefore, for each time step the above set of linear equations have to be solved iteratively.

The equilibrium equation in each time step is solved iteratively by using Newton-Raphson iterative scheme. Similar as in the solution of the thermo-hygrol part of the problem, temperature and pore pressure (humidity) are taken to be constant during the iteration process. In the FE analysis the solution strategy shows relatively poor convergence. There are two reasons for this: (i) the transitional region of the state of the pore water from unsaturated to saturated, which is rather abrupt and (ii) the linearization of coupled equations. To stabilize the numerical solution, time step has to be relatively small. Moreover, in the finite element analysis one has to work with averaged finite element values of temperature, pore pressure and moisture. The averaging is performed over the integration point of a single finite element.

## 4. Numerical studies

### 4.1. Verification of the model implementation

To check the implementation of the model into the 3D finite element code, the example taken from the literature (Bažant and Kaplan 1996) is analyzed and the results are compared. In the example a concrete wall was heated from one side. Two different boundary conditions were considered (see Fig. 2). In the first case (Fig. 2 a,c) the moisture flow at the concrete surface was possible in both directions whereas in the second case (Fig. 2 b,d) the moisture flow was possible

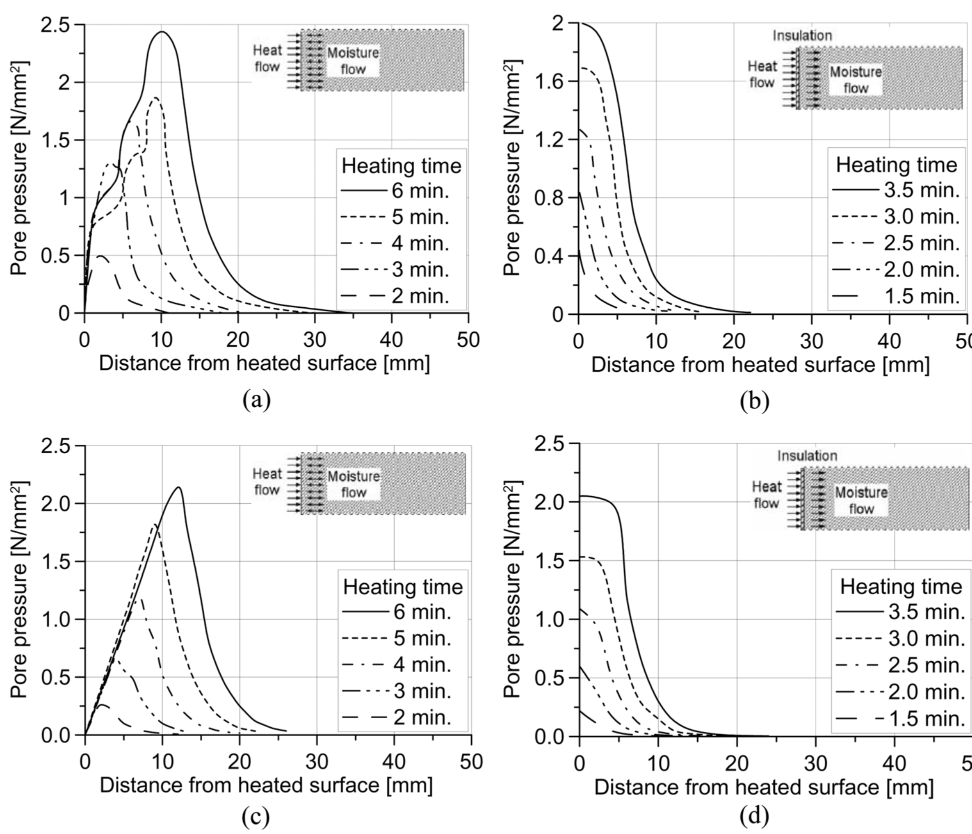


Fig. 2 Distribution of pore pressure for two different boundary conditions at the concrete surface: (a,b) according to Bažant and Kaplan (1996), (c,d) the proposed model

only into concrete wall. The heating rate of 80ºC/min was used and the concrete properties were: thermal conductivity $\lambda$ = 1.67 J/m·sk, initial permeability at 25ºC $a_0 = 10^{-12}$ m/s, saturation water content $w_1$ = 100 kg/m$^3$, water/cement ratio $w/c$ = 0.50 and weight density of concrete $\rho$ = 2400 kg/m$^3$. Calculated are distributions of temperature, pore pressure and moisture. The calculated distribution of pore pressure for both cases is shown in Fig. 2. The results obtained by the presented model (Fig. 2 c,d) are similar to those obtained by Bažant and Kaplan (1996) (Fig. 2 a,b). This confirms that the model is correctly implemented.

### *4.2. Study of explosive spalling of concrete cover*

The proposed thermo-hygro-mechanical model for concrete is employed to investigate explosive spalling of concrete cover. In the numerical example a concrete slab of infinite length is locally heated at free surface (see Fig. 3a). The depth of the slab is 150 mm and the considered width is 480 mm (only symmetric part is analyzed). Varied are concrete strength, porosity, permeability and moisture content. Moreover, the role of geometrical nonlinearity (instability) for the problem of explosive spalling is studied as well. To assure mesh objective results, in the mechanical part of the model the crack band method (Ožbolt, *et al.* 2005) is used. In the analysis eight node solid elements are employed (see Fig. 3b) assuming plane strain condition. Except at the free concrete surface, all

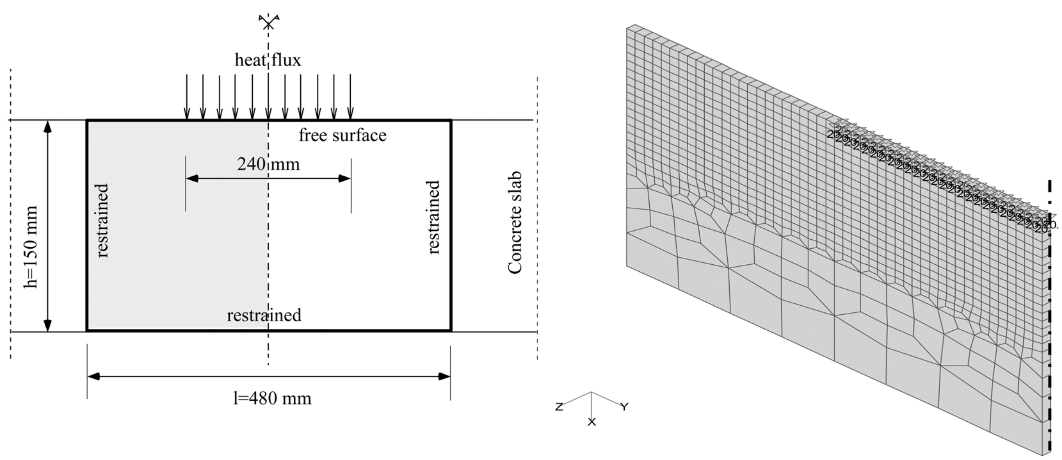


(a) (b)

Fig. 3 Geometry of the heated concrete slab and the corresponding FE model

Table 1 Properties of concrete used in the FE analysis

| | | | |
|---|---|---|---|
| Young's modulus $E$ [MPa] | 30000 | Mass density $\rho$ [kg/m$^3$] | 2400 |
| Poisson's ratio $\nu$ | 0.18 | Water/cement ratio | 0.5 |
| Tensile strength $f_t$ [MPa] | 2.0 | Saturation water content [kg/m$^3$] | 100 |
| Uniaxial comp. strength $f_c$ [MPa] | 30.0 | Parameter $\alpha_a$ | 0.0 |
| Fracture energy $G_F$ [N/mm] | 0.1 | Parameter $\alpha_n$ | 0.375 |
| Conductivity $b$ [J/(ms K)] | 1.67 | Surface emissivity of water $\alpha_w$ | max. |
| Heat capacity $C$ [J/(kg K)] | 900 | Surface emissivity of heat $\alpha_G$ | max. |

boundaries of the specimen are restrained in all three directions. The analysis is static, i.e., structural inertia forces are not accounted for. The linear increase of air temperature in time is applied with a temperature gradient of 80°C/min. Pore pressure at the surface is taken to be 1.0 kN/m$^2$. The analysis is performed for the time period of 12 minutes (duration of heating).

The concrete properties used in the present example of explosive spalling of concrete cover were: initial permeability $a_0 = 10^{-12}$ m/s, humidity $rh_0$ = 75%, initial temperature of concrete $T_0$ = 20°C and initial porosity $n_0$ = 0.10. The remaining parameters were as listed in Table 1. The failure mode, which is typical for explosive spalling is shown in Fig. 4. Fig. 4(a) shows initialization of spalling. The dark zone (maximal mechanical principal strain) shows localization of damage. After initialization complete spalling takes place very quickly. The corresponding failure mode is shown in Fig. 4(b). To understand the failure mechanism, the distribution of macroscopic stresses parallel ($\sigma_y$) and perpendicular ($\sigma_x$) to the free surface at initialization and after spalling are shown in Fig. 5. From Fig. 5(a) it can be seen that because of equilibrium reason the stresses in direction perpendicular to the free surface are almost zero. On the other hand, parallel to the free surface

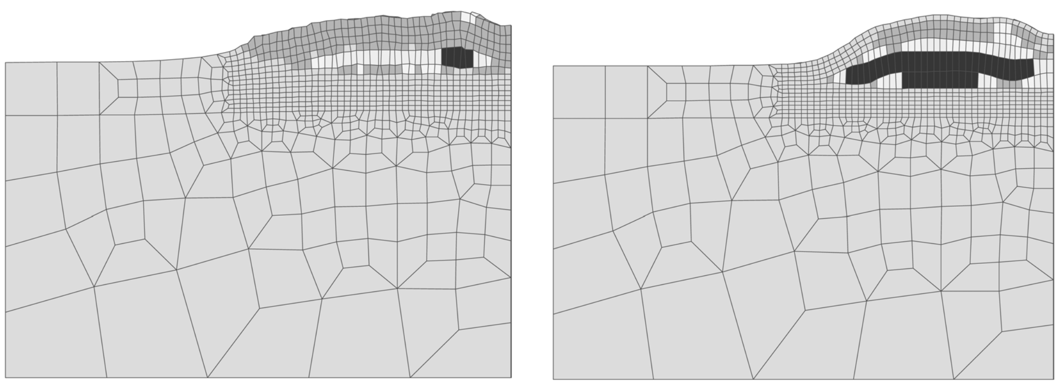

(a) (b)

Fig. 4 a) Localization of damage (max. mechanical principal strains) at initialization of spalling and b) crack pattern due to spalling

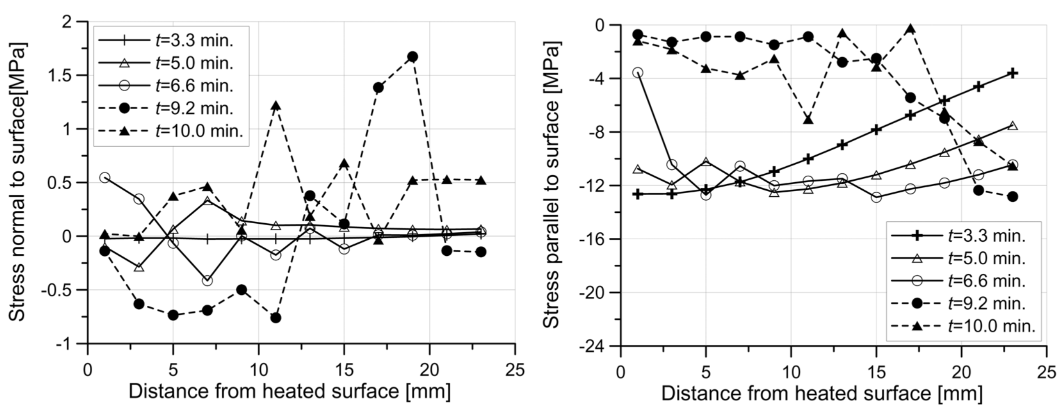


(a) (b)

Fig. 5 Distribution of stresses caused by deformation of concrete before and after spalling: a) in direction perpendicular to concrete surface ($\sigma_x$) and b) in direction parallel to concrete surface ($\sigma_y$)

there are relatively high compressive stresses, which after spalling reduces almost to zero. It turns out that these stresses are not high enough to cause buckling of concrete cover. Namely, the companion numerical analysis, in which pore pressure was not considered, predicts almost the same macroscopic stresses but no spalling. In absence of lateral stresses, which are generated by pore pressure, there is no spalling. Therefore, it can be concluded that in the present example the main driving force for initialization of spalling is pore pressure and not thermal strain induced stresses.

Fig. 6(a) shows the time evolution of pore pressure in the element in which spalling is initialized, before and after (dotted lines) spalling . The relative high pore pressure predicted by the model is supported by a simple engineering approach according to which the critical pore pressure, i.e. pore pressure that corresponds to tensile strength of bulk material (concrete), reads: $p_{crit} = f_t\ (1\text{-}n)/n$. For initial porosity $n$ = 0.1, pore pressure at initialization of spalling is $p_{crit} = 9f_t$. After accounting for the reduction of tensile strength due to high temperature, tensile strength of concrete is in the range of 1.0 to 1.5 MPa. For this strength the critical pore pressure is in the range of 9.0 to 13.5 MPa, which is in good agreement with the outcome of the present model.

In the present example pore pressure, and therefore initialization of spalling, is mainly controlled by permeability of concrete. To illustrate this, the evolution of pore pressure for the initial

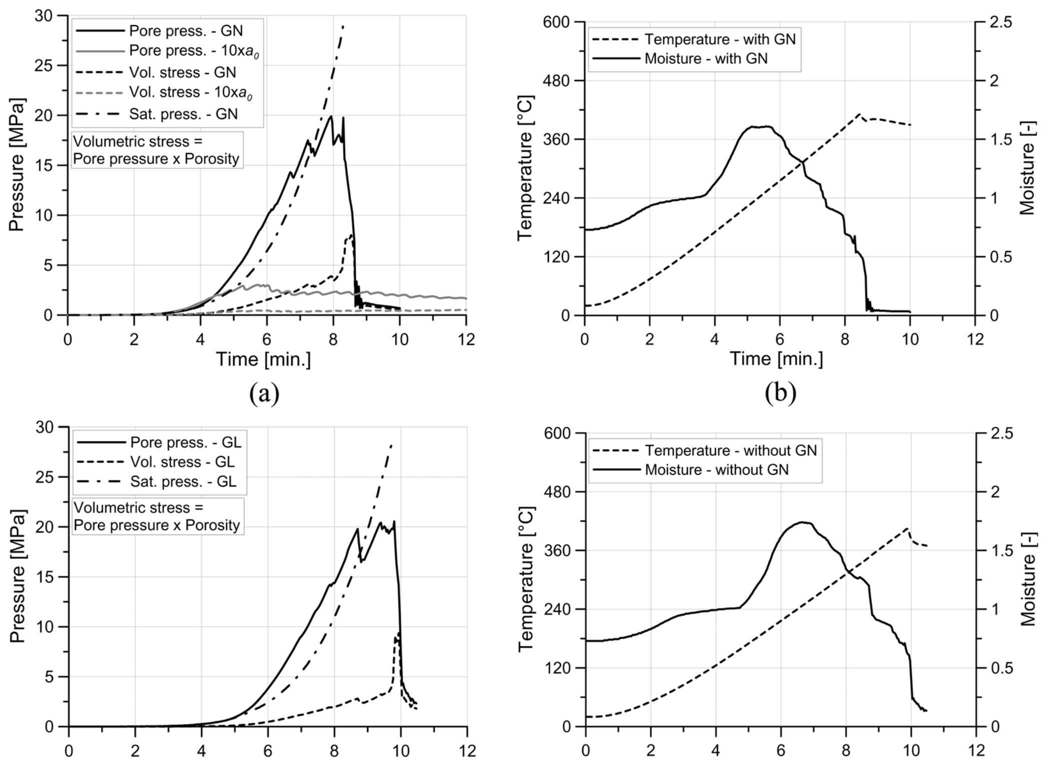


Fig. 6 Time evolution of: a) pore pressure, volumetric stress and saturated pore pressure and b) temperature and humidity in the finite element in which spalling initiates for the case with geometrical non-linearity; c) and d) the same as a) and b) but without geometrical nonlinearity (initial parameters – $a_0 = 10^{-12}$ m/s, $rh_0$ = 75%, $T_0$ = 20ºC and $n_0$ = 0.1)

permeability, which is 10 times larger than the original one, is also shown in Fig. 6(a). Compared to the original case, the maximal pore pressure is reduced by the factor of approximately 5 and therefore no spalling takes place.

In Figs. 6(a), (b) is also plotted the evolution of volumetric stress, temperature, humidity and saturation pressure. In Figs. 6(c), (d) the results are plotted for the analyses without geometrical nonlinearity. It can be seen that the evolution of relevant quantities in the critical section (initialization element) is similar as shown in Figs. 6(a), (b) (geometrical nonlinearity), except that in the analysis with geometrical nonlinearity, spalling initiates earlier and closer to the concrete surface. This clearly indicates that geometrical nonlinearity increases the risk for explosive spalling.

Typical distribution of pore pressure, volumetric stresses, moisture and temperature, as a function of depth is shown in Fig. 7. The results are plotted for time steps before and after spalling (dotted lines). It can be seen that maximal moisture (over saturation) is localized in front of maximal pore pressure. The highest pore pressure and volumetric stresses are generated at crack initiation. After crack propagation (spalling) pore pressure and volumetric stresses abruptly reduce. The pore pressure reduces from approximately 20 MPa at initiation of spalling to 4 MPa at spalling. The volumetric stress drops from 8 MPa to 1 MPa.

Although the presented results are not directly compared with predictions of similar models, it

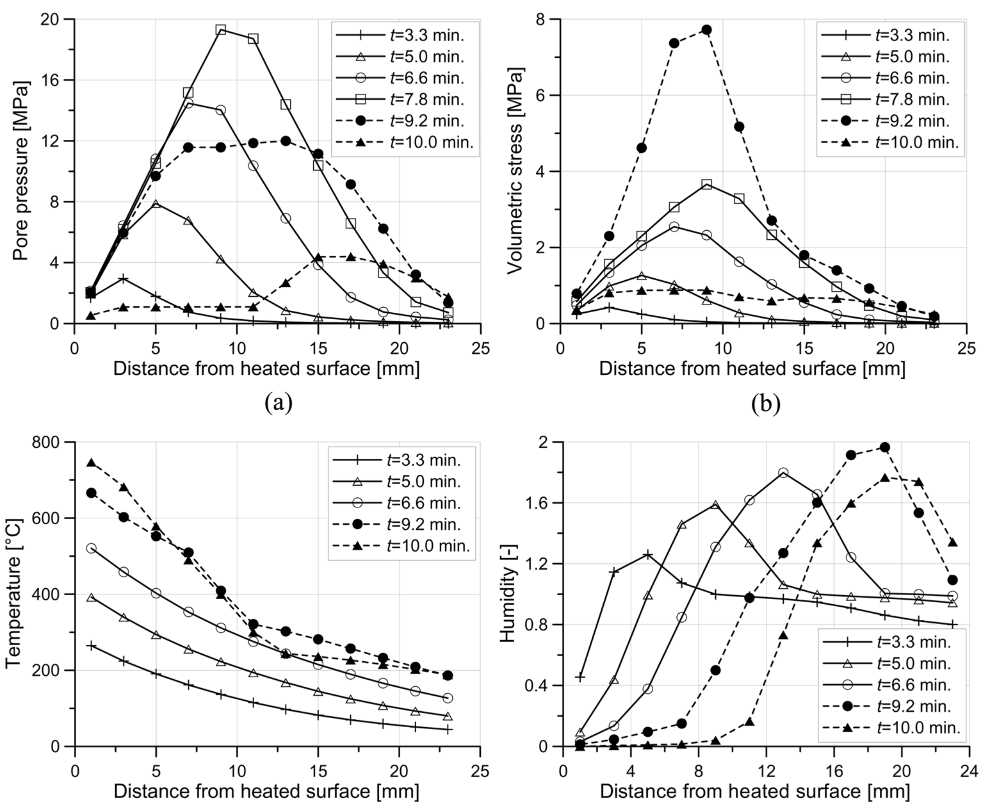


Fig. 7 Distribution of: a) pore pressure, b) volumetric stresses, c) temperature and d) humidity, before and after spalling, measured from the concrete surface (initial parameters – $a_0 = 10^{-12}$ m/s, $rh_0$ = 75%, $T_0$ = 20ºC and $n_0$ = 0.1)

should be mentioned that, based on the literature review (Gawin, *et al*. 1999, 2006, Tenchev, *et al*. 2001), the majority of models principally predict very similar results. The largest discrepancy in the predictions of various models is due to the prediction of pore pressure. For the same or similar material properties and boundary conditions, as used in the present example, the predicted maximal pore pressure in the literature varies from 1 MPa to 10 MPa (Gawin, *et al*. 1999, 2006, Tenchev, *et al*. 2001). Therefore, the results of the present model must be considered as a preliminary, i.e., further work is needed to verify the model and to come up with results, which can bring more light into the mechanisms that govern explosive spalling of concrete cover. This is especially the case for the loading with higher heating rates where besides pore pressure the compressive stresses parallel to free concrete surface, together with geometrical nonlinearity, can strongly influence explosive spalling.

## 5. Conclusions

The paper deals with the modelling of concrete at high temperature. The constitutive model employed in the analysis is formulated in the framework of continuum mechanics taking into account basic principles of irreversible thermodynamics. The main difficulties are related to the identification of material parameters, which are coupled not only in the thermo-hygrol part of the model, but also in the mechanical part of the model. The model is implemented into a 3D finite element code. In the code, the governing thermo-hydro-mechanical equations are solved simultaneously using incremental iterative integration scheme. Subsequently, the model is used in the numerical study of explosive spalling of concrete cover at high temperature.

The study indicate that for the investigated case the main reason for explosive spalling is due to pore pressure. The relatively high pore pressure is generated in front of the over-saturated zone of concrete. It generates high volumetric tensile stresses in concrete, which lead to initiation of cracking. Once the crack initiates there is explosive spalling after which pore pressure and volumetric stresses abruptly reduce. The results show that pore pressure is mainly influenced by permeability of concrete. Furthermore, there is a clear indication that the influence of geometrical instabilities, due to compressive stresses generated parallel to the concrete surface, plays only a secondary role. It is not the main driving force, however, it increases the risk for explosive spalling.

Although, the presented model seems to be promising, further verification of the model and additional numerical studies are needed to clarify the problem of explosive spalling of concrete cover at high temperatures.

## References

Bažant, Z. P. and Cusatis, G. (2005), "Concrete creep at high temperature and its interaction with fracture: Recent progress", *CONCREEP-7*, Ed. Pijaudier-Cabot, Gerard & Acker, Hermes Science, 449-460.

Bažant, Z. P. and Kaplan, M. F. (1996), *Concrete at High Temperatures: Material Properties and Mathematical Models*, Harlow, Longman.

Bažant, Z. P. and Thonguthai W. (1978), "Pore pressure and drying concrete at high temperature", *ASCE J. Eng. Mech.*, **104**, 1059-1079.

Belytschko, T., Liu, W. K. and Moran, B. (2001), *Nonlinear Finite Elements for Continua and Structures*, John Wiley & Sons Ltd.

Gawin, D., Majorana, C. E. and Schrefler, B. A. (1999), "Numerical analysis of hygro-thermal behavior and damage of concrete at high temperature", *Mechanics of Cohesive Frictional Materials*, **4**, 37-74.

Gawin, D., Pesavento, F. and Schrefler B. A. (2006), "Towards prediction of the thermal spalling risk through a multi phase porous media model of concrete", *Comput. Methods Appl. Mech. Eng*., **195**, 5707-5729.

Harmathy, T. Z. and Allen, L. W. (1973), "Thermal properties of selected masonry unit concretes", *J. Amer. Inst.*, **70**, 132-144.

Khoury, G. A., Grainger, B. N. and Sullivan, P. J. E. (1985), "Transient thermal strain of concrete: literature review, conditions within specimens and behaviour of individual constituents", *Mag. Concrete Res*., **37**(132), 131-144.

Khoury, G. A. (2006), "Strain of heated concrete during two thermal cycles – Parts 1,2 and 3", *Mag. Concrete Res.*, **58**(6), 367-385, **58**(6), 387-400 and **58**(7), 421-435.

Nielsen, C. V., Pearce, C. J. and Biani, N. (2002), "Theoretical model of high temperature effects on uniaxial concrete member under elastic restraint", *Mag. Concrete Res*., **54**(4), 239-249.

Ožbolt, J., Li, Y.-J. and Kožar, I. (2001), "Microplane model for concrete with relaxed kinematic constraint", *Int. J. Solids Struct.*, **38**, 2683-2711.

Ožbolt, J., Kožar, I., Eligehausen, R. and Periškić, G. (2005), "Three-dimensional FE analysis of headed stud anchors exposed to fire", *Comput. Concrete*, **2**(4), 249-266.

Schneider, U. (1986), *Properties of Materials at High Temperatures, Concrete*, 2nd. Edition, RILEM Technical Comitee 44-PHT, Technical University of Kassel, Kassel.

Tenchev, R. T., Li, L. Y. and Purkiss, J. A. (2001), "Finite element analysis of coupled heat and moisture transfer in concrete subjected to fire", *Numerical Heat Transfer*, **39**, 685-710.

Thelandersson, S. (1983), "On the multiaxial behaviour of concrete exposed to high temperature", *Nucl. Eng. Design*, **75**(2), 271-282.

Therrien, R. and Sudicky, E. A. (1996), "Three-dimensional analysis of variably-saturated flow and solute transport in discretely-fractured porous media", *J. Contaminant Hydrology*, **23**(1-2), 1-44.

Wang, K., Jansen, D. C. and Shah, P. S. (1997), "Permeability study of cracked concrete", *Cement Concrete Res.*, **27**(3), 381-393.

Zhang, B. and Bićanić, N. (2002), "Residual fracture toughness of normal- and high-strength gravel concrete after heating to 600°C", *ACI Mater J*., **99**(3), 217-226.

Zieml, M., Leithner, D., Lackner, R. and Mang, H. A. (2006), "How do polypropylene fibers improve the spalling behavoiur of in-situ concrete", *Cement Concrete Res*., **36**(5), 929-942.